

# A Skeletal Symmetry Index for Patient Derived Quantitative Quality Control in $^{99m}\text{Tc}$ -MDP Bone Scintigraphy

<sup>1</sup>Sudipto Das, <sup>1</sup>Kazi Reazuddin Ahmed, <sup>2</sup>Md. Jahir Alam, <sup>3</sup>Ilteza Tabassum, <sup>3</sup>Moontaha Binte Rashid, <sup>2</sup>Mahbuba Zaman, <sup>3</sup>Jerin Sultana, <sup>4</sup>Afroza Naznin, <sup>5</sup>Azmal Kabir Sarker, <sup>6</sup>Zeenat Jabin

<sup>1</sup>Scientific Officer, Institute of Nuclear Medicine and Allied Sciences (INMAS), Suhrawardy

<sup>2</sup>Scientific Officer, INMAS, Mohakhali, Dhaka

<sup>3</sup>Medical Officer, <sup>4</sup>Senior Medical Officer, <sup>5</sup>Principal Medical Officer, <sup>6</sup>Director & CMO, INMAS, Suhrawardy

**Correspondence Address** : : Sudipto Das, Scientific Officer, INMAS, Suhrawardy, ShSMCH Campus, Sher-E-Bangla Nagar, Dhaka- 1207, E-mail: physudip43@gmail.com

## ABSTRACT

**Introduction:** This study utilizes the Skeletal Symmetry Index (SSI) to quantify bilateral uptake uniformity of  $^{99m}\text{Tc}$ -MDP bone scintigraphy images, aiming to compare calculated values with previously published reference limits to differentiate physiological variation.

**Method:** Bone scintigraphy data of 35 adult patients were analyzed retrospectively across five anatomical regions: skull, humerus, rib, iliac crest, and femur. Bilateral asymmetry was quantified using the mentioned SSI formula. Standard statistical analysis was performed to analyze and correlate the regional count data.

**Results:** High degrees of bilateral symmetry were observed across all skeletal sites. The calculated SSI values (median) ranged from 2.12% (skull) to 7.28% (humerus). Spearman's correlation showed exceptionally strong symmetry. Most of the regions showed random count variation, but the regional count of ribs exhibited a statistically significant right-sided prevalence in the Wilcoxon signed-ranks test, likely due to hepatic activity. All measured indices remain well below the 10% clinical threshold for pathological asymmetry.

**Conclusion:** SSI confirms high skeletal symmetry that is well below previously published limits and serves as a practical tool for routine image quality control.

**Keywords:** Quantitative imaging, uniformity, skeletal symmetry,  $^{99m}\text{Tc}$ -MDP bone scintigraphy.

## INTRODUCTION

Bone scintigraphy with the use of  $^{99m}\text{Tc}$  Methylene Diphosphonate ( $^{99m}\text{Tc}$ -MDP) is a well-established nuclear medicine technique for the assessment of bone metabolism and pathology. The procedure is based on the principle of the preferential uptake of the radiopharmaceutical in areas of active bone metabolism, which is indicative of osteoblastic activity and blood flow. Due to the high sensitivity of the procedure, whole-body bone scintigraphy is of primary importance in the detection of metastatic disease, trauma, infections, and metabolic bone diseases. The final image is indicative of the spatial distribution of the counts detected, which is a result of fundamental physical laws such as radioactive decay, attenuation of photons, scatter, etc.

This study uses a practical quantitative approach to evaluate skeletal uptake symmetry in whole-body bone scintigraphy by introducing a Skeletal Symmetry Index (SSI), calculated from the relative difference in counts between corresponding regions on the left and right sides of the body. The aim is to move beyond subjective visual assessment and determine how reliably symmetry can be measured using routine clinical images, while also examining how this symmetry varies across different skeletal regions. Rather than assuming perfect bilateral equivalence, the study acknowledges inherent physiological variation and places measured asymmetry in the context of system performance by comparing it with the known uniformity limits of the gamma camera. In doing so, it establishes a lower boundary below which observed differences are more likely attributable to

detector non-uniformity than true biological variation. By combining simple count-based analysis with fundamental imaging physics, this work reframes skeletal symmetry as a measurable parameter with defined limits, offering a more objective and standardized basis for interpreting bone scintigraphy in clinical practice.

Quantitative assessment of skeletal symmetry in nuclear medicine has been explored in multiple contexts, establishing a foundation for objective interpretation beyond conventional visual analysis. Early work in bone scintigraphy introduced computer-aided sacroiliac joint indices and quantitative left–right uptake comparisons to support clinical evaluation, demonstrating both feasibility and clinical relevance (1–3). Asymmetry scores have also been applied in three-phase bone scintigraphy—for example, in the evaluation of complex regional pain syndrome—where quantitative bilateral differences enhanced diagnostic sensitivity (4). Although these approaches highlight the utility of symmetry metrics, they largely focus on specific applications rather than standardized skeletal frameworks. Evidence from related fields further underscores that perfect bilateral symmetry is rarely observed: investigations of hip bone mineral density reveal strong correlations but measurable physiological variation independent of age, emphasizing the need to consider natural asymmetry when defining normal limits (5, 6). Methodological studies from biomechanics and movement analysis illustrate how symmetry indices can be rigorously normalized and standardized, demonstrating that index choice and formulation significantly influence quantification outcomes (7–9). Additionally, clinical studies incorporating sacroiliac indices have shown improved specificity in scintigraphic diagnosis, supporting the practical value of bilateral quantification (10). Collectively, these works provide a compelling rationale for developing a quantitative, region-specific skeletal symmetry index that accounts for inherent biological variation while integrating imaging physics. Despite prior efforts, a comprehensive framework that establishes normal reference limits across skeletal regions and distinguishes physiologic from system-related asymmetry remains absent, motivating the present study to extend existing symmetry index concepts into a

whole-skeleton, region-specific framework for routine clinical QC, which has not been systematically explored.

In this study, we used routinely acquired bone scintigraphy data to retrospectively assess skeletal symmetry. We described baseline symmetry patterns and their variability under typical clinical conditions by examining bilateral regions of interest across several anatomical sites. In addition to traditional phantom-based quality assurance, the skeletal symmetry index offers a straightforward, quantitative measure that represents image uniformity and system performance. Bone scintigraphy can be interpreted more intelligently using these patient-derived metrics, which provide an additional viewpoint on imaging consistency. All things considered, this work shows how symmetry-based analysis can be used practically and emphasizes how it could improve quantitative evaluation and quality control in nuclear medicine.

## METHODOLOGY

The study sample consisted of 35 adult individuals ( $n=35$ ), who underwent bone scintigraphy in our nuclear medicine institute. Patients with high pathological uptake and skeletal metastasis are excluded from the study. Whole body  $^{99m}\text{Tc}$ -MDP bone scintigraphy was performed using a Mediso AnyScan S dual-head SPECT system. The system was equipped with low energy high resolution (LEHR) parallel hole collimators using 140 keV peak energy and a 20% energy window. Images were acquired in a continuous scanning mode into a matrix with a pixel size of 2.74 mm and a zoom factor of 0.89. The scan speed was set to 150 mm/min. A standard dosing protocol (300-740 MBq) and 3 h of uptake time were maintained.

Five anatomical regions were selected for bilateral symmetry analysis: the skull, humerus, rib, iliac crest, and femur. Counts were recorded for both the left (L) and right (R) sides, drawing simple circular regions of interest (ROIs) to ensure replicability. The right-sided ROIs are drawn duplicating the left-sided ROIs to maintain uniformity. ROIs are placed on specifically proximal third of the humerus and femur, 10th rib and parietal bones of the skull. All the ROIs are drawn in the posterior aspect of the bone scintigraphy image.

Skeletal symmetry was quantified using a skeletal symmetry index (SSI) to allow for normalized comparison across different skeletal dimensions. The index was calculated according to the following formula (11)

$$SSI\% = \frac{|Counts_L - Counts_R|}{\frac{1}{2}(Counts_L + Counts_R)} \times 100 \quad (1)$$

This index expresses the absolute difference between sides as a percentage of the individual's mean size, effectively controlling for overall body size scaling. An SSI value of 0 indicates perfect bilateral symmetry, while higher values represent increasing degrees of fluctuating or directional asymmetry. After calculating all the indices, standard statistical tests (data distribution and correlation analysis) were performed using IBM SPSS v26 software.

## RESULTS AND DISCUSSION

The study included a cohort of 35 routine  $^{99m}Tc$ -MDP bone scintigraphy patients. Patient demographics are listed in **Table 1**. The mean age of the patients is years. The range of age (20 years – 95 years) indicates a wide variation in adult individuals included in this study. But the study population is predominantly female (62.86%), while males represented 37.14% of the population. This female predominance is quite common in bone scintigraphy, as mentioned in several previous studies (12, 13).

**Table 1: Patient Demographics**

Number of Patients	35
Age (Mean ± SD)	54.97±16.46
Age Range	(20-95)
Male (n, %)	13, 37.14%
Female (n, %)	22, 62.86%

All the count data are extracted from five skeletal ROIs, and the corresponding skeletal symmetry index is calculated according to the formula mentioned in the methodology section. The count data for these regions, including medians and IQRs, are summarized in **Table 2**. The highest median counts are observed in the skull, while the humerus exhibited the lowest median count density. Generally, the median values for the left and cardiac sides across all anatomical sites appeared closely

aligned, suggesting a high degree of bilateral uniformity in tracer uptake or physiological activity.

**Table 2: Count Data of ROI at five different skeletal sites.**

Anatomical Site	Side	Median	IQR (25 <sup>th</sup> -75 <sup>th</sup> )
Skull	Left	4564	(3069-7958)
	Right	4933	(3141-7970)
Humerus	Left	2666	(1804-3228)
	Right	2644	(1953-3151)
Rib	Left	4572	(2694-5354)
	Right	4712	(2713-5710)
Iliac crest	Left	3916	(3383-6092)
	Right	4035	(3076-6282)
Femur	Left	4323	(2920-5457)
	Right	4028	(2977-5632)

Before statistical analysis, the distribution of count data and calculated SSI across all the five skeletal regions is evaluated, which is a crucial preliminary procedure of medical data analysis (14). Based on data normality assessment, the majority of the variables, including SSI for skull, humerus, and ribs, exhibited significant deviation from a normal distribution. Visual inspection of the histogram and Q-Q plots further confirmed a non-normal distribution showing varying degrees of skewness. As the data is non-normal, the median (IQR) is used for standard representation of data rather than the mean. Also, Spearman's rank correlation coefficient is used to assess the strength of bilateral relationships between bilateral counts, and the Wilcoxon signed-ranks test was utilized to determine the significance of the difference between anatomical pairs (15).

To evaluate the strength of the relationship between bilateral pairs, Spearman's rank correlation coefficient is calculated. The result demonstrates exceptionally strong and statistically significant correlation across all five pairs at this level. The degree of symmetry is observed as skull > femur > iliac crest > humerus. The scatter plots (**Figure 1**) further visually confirmed this degree of symmetry. A narrow confidence interval (red shaded region around the regression line) is seen at the femur and skull, showing nearly a perfect symmetry. The other three regions show a wider confidence interval that is consistent with Spearman's rank correlation test.

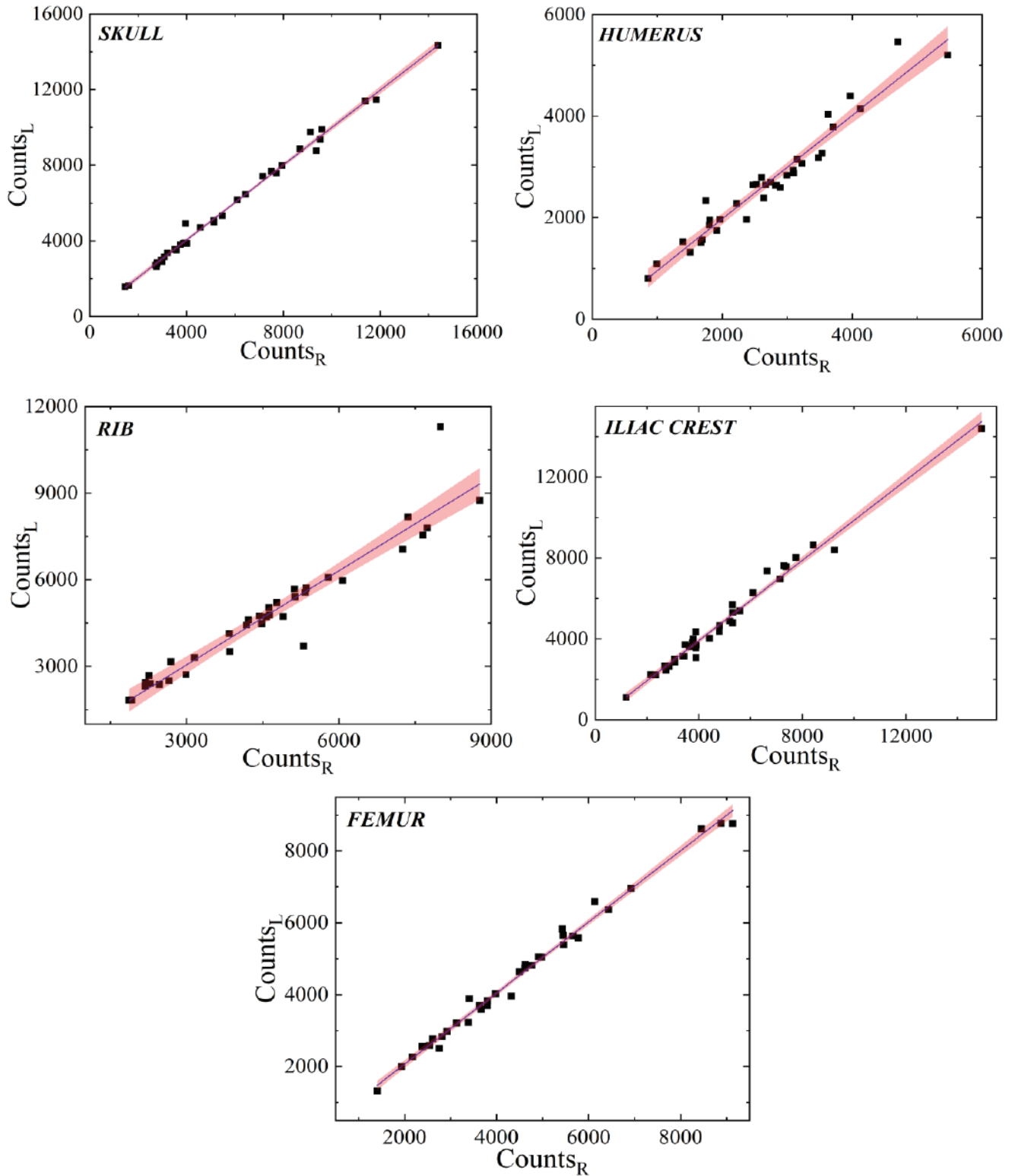


**Figure 1: Bilateral counts of five skeletal regions (skull, humerus, rib, iliac crest and femur)**

The SSIs are calculated and visually represented in a box plot diagram (**Figure 2**). The median SSI% values remained low across all sites: skull (2.12%), humerus (7.28%), rib (5.22%), iliac crest (6.05%), and femur

(2.62%). The box plot illustrates that the skull and femur show the highest precision (narrowest IQR and lowest SSI), while the humerus and rib exhibit slightly higher variability and a number of outliers. Slightly higher

asymmetry in the humerus and ribs is quite common in adult individuals due to left- or right-hand dominance and the presence of the liver under the rib cage (16, 17). In our study, the right-sided counts in the rib are slightly higher than the left (due to the hepatic count on the right side).

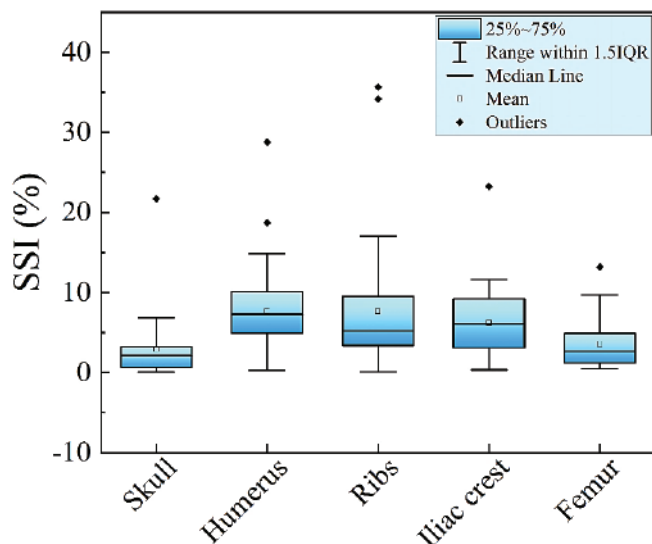


**Figure 2: Percentage of symmetry index for five anatomical sites**

To further compare among the five regions, a Wilcoxon signed-rank test is performed. The analysis revealed no statistically significant differences in bilateral counts for the skull, humerus, iliac crest, and femur, indicating that any observed variation in these regions is likely random. However, a significant difference is observed in the rib, where the positive rank (predominance) is consistent with the data presented in This study validates a high degree of bilateral skeletal symmetry, establishing a robust quantitative baseline for using contralateral regions as internal controls in nuclear medicine. This physiological synchronization is further validated by the technical performance of the imaging system, which maintained an integral uniformity of 1.8% and a differential uniformity of 1.3% across both the useful field of view (UFOV) and central field of view (CFOV) using a  $^{99m}\text{Tc}$  flood source. These QC metrics ensure that the observed SSIs (ranging from 2% to 7%) reflect true biological distribution rather than detector non-uniformity. While the skull and femur showed the highest levels of symmetry. According to previous studies, a quantitative difference in radiotracer uptake of less than 10% between contralateral skeletal structures is considered within the range of normal

physiological variation, whereas a threshold of 10% or greater is typically required to indicate clinically significant asymmetry (18, 19). So, the exceptional performance of our imaging system, coupled with a Skeletal Symmetry Index (SSI) of 2–7%, demonstrates that our findings remain well below the established 10% clinical threshold for pathological asymmetry.

## CONCLUSION

This study successfully demonstrates that bilateral count symmetry in  $^{99m}\text{Tc}$ -MDP bone scintigraphy serves as a practical, patient-derived tool for checking gamma camera performance. By quantifying tracer distribution across corresponding skeletal regions, the research confirms that routine clinical data can effectively monitor system uniformity and identify technical inconsistencies. Ultimately, this approach proves that symmetry-based analysis provides a reliable, objective method for verifying imaging integrity alongside traditional quality control protocols.

## REFERENCES

- Huang JY, Tsai MF, Kao PF, Chen YS. Automatic computer-aided sacroiliac joint index analysis for bone scintigraphy. *Comput Methods Programs Biomed.* 2010 Apr; 98(1):15–26.
- Tiwari BP, Basu S. Estimation of sacroiliac joint index in normal subjects of various age groups: comparative evaluation of four different methods of quantification in skeletal scintigraphy. *Nucl Med Rev Cent East Eur.* 2013; 16 (1):26–30.
- Kaçar G, Kaçar C, Karayalçın B, Güngör F, Tuncer T, Erkiliç M. Quantitative sacroiliac joint scintigraphy in normal subjects and patients with sacroiliitis. *Ann Nucl Med.* 1998 Jun; 12(3):169–73.
- Sampath S, Mittal BR, Arun S, Sood A, Bhattacharya A, Sharma A. Usefulness of asymmetry score on quantitative three-phase bone scintigraphy in the evaluation of complex regional pain syndrome. *Indian J Nucl Med IJNM Off J Soc Nucl Med India.* 2013; 28(1):11–6.
- Lessig HJ, Meltzer MS, Siegel JA. The symmetry of hip bone mineral density. A dual photon absorptiometry approach. *Clin Nucl Med.* 1987 Oct; 12(10):811–2.
- Yang RS, Chieng PU, Tsai KS, Liu TK. Symmetry of bone mineral density in the hips is not affected by age. *Nucl Med Commun.* 1996 Aug; 17(8):711–6.
- Queen R, Dickerson L, Ranganathan S, Schmitt D. A novel method for measuring asymmetry in kinematic and kinetic variables: The normalized symmetry index. *J Biomech.* 2020 Jan 23; 99:109531.
- Siebers HL, Alrawashdeh W, Betsch M, Migliorini F, Hildebrand F, Eschweiler J. Comparison of different symmetry indices for the quantification of dynamic joint angles. *BMC Sports Sci Med Rehabil.* 2021 Oct 19; 13:130.
- Pierre MA, Zurakowski D, Nazarian A, Hauser-Kara DA, Snyder BD. Assessment of the bilateral asymmetry of human femurs

- based on physical, densitometric, and structural rigidity characteristics. *J Biomech.* 2010 Aug 10; 43(11):2228–36.
10. Koç ZP, Cengiz AK, Aydın F, Samancı N, Yazısız V, Koca SS, et al. Sacroiliac Indicators Increase the Specificity of Bone Scintigraphy in the Diagnosis of Sacroiliitis. *Mol Imaging Radionucl Ther.* 2015 Feb; 24(1):8–14.
  11. Brinkmann BH, Jones DT, Stead M, Kazemi N, O'Brien TJ, So EL, et al. Statistical Parametric Mapping Demonstrates Asymmetric Uptake with Tc-99m ECD and Tc-99m HMPAO SPECT in Normal Brain. *J Cereb Blood Flow Metab.* 2012 Jan 1; 32(1):190–8.
  12. Assessment of effects induced by bone scintigraphy dose in red & white blood cells relative to ageing and obesity. *MOJ Public Health.* 2020 Sep 30; Volume 9(Issue 5).
  13. Hosen MA, Begum N, Hossain M, Ahmed P, Mutsuddy P, Chowdhury SA. Tc-99m MDP Bone Scan Evaluation in Breast Cancer: A Study on 425 Patients. *Med Today.* 2018 Aug 8; 30(2):49–52.
  14. Ghasemi A, Zahediasl S. Normality Tests for Statistical Analysis: A Guide for Non-Statisticians. *Int J Endocrinol Metab.* 2012; 10(2):486–9.
  15. Nahm FS. Nonparametric statistical tests for the continuous data: the basic concept and the practical use. *Korean J Anesthesiol.* 2016 Feb; 69(1):8–14.
  16. Irish M. Adult Human Rib Variation of Symmetry Among Many Populations. Williams Honors College, Honors Research Projects, 2025. (Dissertation).
  17. Dare SS, Masilili G, Mugagga K, Ekanem PE. Evaluation of Bilateral Asymmetry in the Humerus of Human Skeletal Specimen. *BioMed Res Int.* 2019 Jul 16; 2019:3194912.
  18. Saridin CP, Raijmakers PGHM, Tuinzing DB, Becking AG. Comparison of planar bone scintigraphy and single photon emission computed tomography in patients suspected of having unilateral condylar hyperactivity. *Oral Surg Oral Med Oral Pathol Oral Radiol Endodontology.* 2008.
  19. Saridin CP, Raijmakers PGHM, Tuinzing DB, Becking AG. Bone scintigraphy as a diagnostic method in unilateral hyperactivity of the mandibular condyles: a review and meta-analysis of the literature. *Int J Oral Maxillofac Surg.* 2011 Jan; 40(1):11–7.